Imaging of Tumor Hypoxia With ^{18}F-EF5 PET/MRI in Cervical Cancer

Sara I. Narva, MD,*† Marko P. Seppänen, MD, PhD,†‡ Juho R.H. Raiko, MD, PhD,†‡ Sarita J. Forsback, MS, PhD,†‡ Katri J. Orte, MD, PhD,†§ Johanna M. Virtanen, MD, PhD,†∥ Johanna Hynninen, MD, PhD,*† and Sakari Hietanen, MD, PhD*†

Purpose of the Report: The aim of this study was to evaluate the distribution of hypoxia using ^{18}F-EF5 as a hypoxia tracer in cervical cancer patients with PET/MRI. We investigated the association between this ^{18}F-EF5-PET tracer and the immunohistochemical expression of endogenous hypoxia markers: HIF1α, CAIX, and GLUT1.

Patients and Methods: Nine patients with biopsy-proven primary squamous cell cervix carcinoma (FIGO 2018 radiological stages IB1–IIIC2r) were imaged with dual tracers ^{18}F-EF5 and ^{18}F-FDG using PET/MRI (*Int J Gynaecol Obstet.* 2019;145:129–135). ^{18}F-EF5 images were analyzed by calculating the tumor-to-muscle ratio to determine the hypoxic tissue (T/M ratio >1.5) and further hypoxic subvolume (HSV) and percentage hypoxic area. These ^{18}F-EF5 hypoxic parameters were correlated with the size and localization of tumors in ^{18}F-FDG PET/MRI and the results of hypoxia immunohistochemistry.

Results: All primary tumors were clearly ^{18}F-FDG and ^{18}F-EF5 PET positive and heterogeneously hypoxic with multiple ^{18}F-EF5–avid areas in locally advanced cancer and single areas in clinically stage I tumors. The location of hypoxia was detected mainly in the periphery of tumor. Hypoxia parameters ^{18}F-EF5 max T/M ratio and HSV in primary tumors correlated independently with the advanced stage ($P = 0.036$ and $P = 0.040$, respectively), and HSV correlated with the tumor size ($P = 0.027$). The location of hypoxia in ^{18}F-EF5 imaging was confirmed with a higher hypoxic marker expression HIF1α and CAIX in tumor fresh biopsies.

Conclusions: The ^{18}F-EF5 imaging has promising potential in detecting areas of tumor hypoxia in cervical cancer.

Key Words: EF5, PET/MRI, hypoxia, cervical cancer, immunohistochemistry

(*Clin Nucl Med* 2021;46: 952–957)

H ypoxia is a consequence of an imbalance between supply and consumption of oxygen. It means very low physiologic tissue oxygen levels in tumors (<5 mm Hg) compared with healthy tissues (40–60 mm Hg). In the 1990s, clinical studies assessing oxygen tension (PO₂) in tumors using oxygen needle sensors (Eppendorf method) demonstrated that hypoxia is a common feature of cervical cancer with intertumor and intratumor variability.[1] Hypoxia, both acute and chronic, causes changes in the tumor microenvironment. Cellular adaptation to hypoxia leads to genetic instability and mutagenesis by impaired DNA damage response. This results a more aggressive tumor phenotype and risk for invasion and metastasis. Therefore, hypoxia is associated with a poor prognosis in cervical cancer, regardless of treatment modality.[2]

Today, the best methods for cervical cancer staging are with MRI and ^{18}F-FDG PET combined with hybrid scanners. The integrated PET/MRI was introduced for clinical use in 2011, and its advantages are combining the anatomic, functional, and metabolic tumor characteristics in a single image session for patients with less time and radiation.[3] To visualize the extent of tumor hypoxia on a patient basis with a noninvasive method, novel PET radiotracers have been developed. [18]Fluorine-labeled 2-(2-nitro-1-*H*-imidazol-1-y)-*N*-(2,2,3,3,3-pentafluoropropyl)-acetamide (^{18}F-EF5) is hypoxia tracer with high lipophilicity and good cell membrane permeability. It has slow blood clearance, which improves the rates of tumor uptake and the homogeneity of tracer distribution.[4] ^{18}F-EF5 synthesis was demonstrated in 2001,[5] and the first clinical study for ^{18}F-EF5 PET imaging to identify hypoxia in head and neck cancer was reported by Komar et al[6] in 2008. They also showed that a higher uptake of ^{18}F-EF5 had a stronger correlation with poor clinical outcome than ^{18}F-FDG uptake.[7] Although ^{18}F-EF5 is well validated in preclinical studies and a widely investigated tracer of tumor hypoxia in sarcomas, head and neck cancer, and brain tumors, little is known about clinical imaging ^{18}F-EF5 PET/MRI in cervical cancer patients.[1]

Tumor hypoxia can be measured reliably with immunohistochemistry (IHC) staining. Hypoxia-inducible factor 1 alpha (HIF1α) and its targeted gene markers glucose transporter 1 (GLUT1) and carbonic anhydrase IX (CAIX) are reported to be highly expressed in cervical cancer and associated with poor prognosis.[8] Immunohistochemistry requires a tumor biopsy and does not represent the oxygenation status of the entire tumor. Therefore, noninvasive molecular imaging techniques could overcome these challenges in evaluating tumor hypoxia in a clinical setting.

In this study, we combined these methods to evaluate tumor hypoxia in patients with primary SCC of the cervix uteri with ^{18}F-EF5 PET/MRI and validated our findings with hypoxia-specific IHC biomarkers.

PATIENTS AND METHODS

Patients

This is a prospective, single-institution feasibility study conducted in Turku University Hospital, Finland. The study was approved by the local ethics committee under the Helsinki Declaration. All 9 patients with newly diagnosed squamous cell carcinoma of cervix uteri provided written informed consent. The clinical characteristics of the

TABLE 1. Characteristics of Patient of Squamous Cell Carcinoma of the Cervix

Patient No.	Age, y	Tumor Gradus	Clinical FIGO Stage	^{18}F-FDG PET/MRI TNM FIGO 2018	^{18}F-FDG PET/MRI Tumor Size, mm	^{18}F-FDG PET/MRI Locally Advanced	^{18}F-FDG PET/MRI LNM	Radical Operation	Primary Chemoradiotherapy
1	46	2	1b1	T1b1N0M0	18	Neg	Neg	+	−
2	54	2	1b2	T3c2rN0M1	58	Neg	Pos	−	+
3	36	3	1b2	T3c1rN1M0	41	Neg	Pos	−	+
4	77	2	2a1	T3aN0M0	57	Pos	Neg	−	+
5	75	2	3a	T3c1rN1M0	62	Pos	Pos	−	+
6	59	3	1b1	T1b2N0M0	31	Neg	Neg	+	−
7	39	2	1b2	T1b2N0M0	38	Neg	Neg	+	−
8	33	2	2b	T3c1rN1M0	66	Pos	Pos	−	+
9	69	3	2a1	T2a2N0M0	50	Pos	Neg	−	+
Mean ± SD	54 ± 16				47 ± 16	Pos 4/9	Pos 4/9	+3/9	+6/9

patients are presented in Table 1. The patients underwent dual tracer imaging with ^{18}F-EF5 and ^{18}F-FDG PET/MRI, the latter being part of the pretreatment staging protocol in our institution for all cervical cancer patients since January 2013. The average interval between different tracer scans was 5.3 days (range, 1–22 days), and they were performed in random order.

Imaging

Synthesis of ^{18}F-EF5

^{18}F-EF5 was synthesized from precursor 2-(2-nitro-1-*H*-imidazol-1-y)-*N*-(2,3,3-trifluoroallyll)-acetamide using high-specific radioactivity ^{18}F-F2 as the labeling reagent.[9] The specific radioactivity of ^{18}F-EF5, decay-corrected to the end of synthesis, exceeded 3.7 GBq/μmol or 10 mCi/μmol.

PET/MRI Device

Data Acquisition Protocol

The both ^{18}F-FDG and ^{18}F-EF5 PET/MRI were performed at the Turku PET Centre (Ingenuity TF PET/MRI; Philips Medical System, Cleveland, OH). The catheter was placed to empty the bladder during PET imaging. IV injection of ^{18}F-EF5 (370 MBq or 10 mCi) was administered 180 minutes before the start of acquisition. Two bed positions of the whole pelvis were acquired to cover the entire pelvic area. MR-based attenuation correction was performed using the vendor-provided method. T2-weighted images were obtained for acquiring MRI data using a single-shot turbo spin-echo sequence. Detector dead time, radioactivity decay, random scatter, and photon attenuation were corrected to the PET data.

The ^{18}F-FDG PET/MRI was performed according to the general clinical routine from the base of skull to mid-thigh. A dose of 370 MBq or 10 mCi of ^{18}F-FDG was injected, and images were acquired in the craniocaudal direction starting 60 minutes from injection.

Image Analysis

All images were interpreted with the medical imaging software Carimas 2.0 (Turku PET Centre, Finland). In FDG images, the tumor FDG uptake was quantified by SUV_{max}, and metabolically active tumor volume (MATV) was determined using 50% of the SUV_{max} as the threshold. High tracer activity in the urine bladder was digitally masked when needed to enable analysis of nearby tissues. The ^{18}F-EF5 images were superimposed over the respective ^{18}F-FDG images to copy the volumes of interest (VOIs) drawn in the FDG images to the EF5 images.

The ^{18}F-EF5 tumor-to-muscle (T/M) uptake ratios were determined by dividing all the voxel SUV_{max} values by the mean muscle SUV_{max} obtained from the VOI covering the gluteus maximus muscle area contralateral to the tumor in 3 consecutive axial PET image slices. The ^{18}F-EF5–avid volume was determined using a T/M ratio threshold greater than 1.5. The total volume of voxels above this threshold and inside the MATV was considered hypoxic subvolume (HSV). Percentage hypoxic area (PHA) was calculated by dividing the summed volume of voxels above the selected T/M threshold by MATV.

Immunohistochemistry and Scoring

Paraffin-embedded 4-μm tissue sections were stained with antibodies raised against CAIX (ab15086; Abcam, Cambridge, United Kingdom,
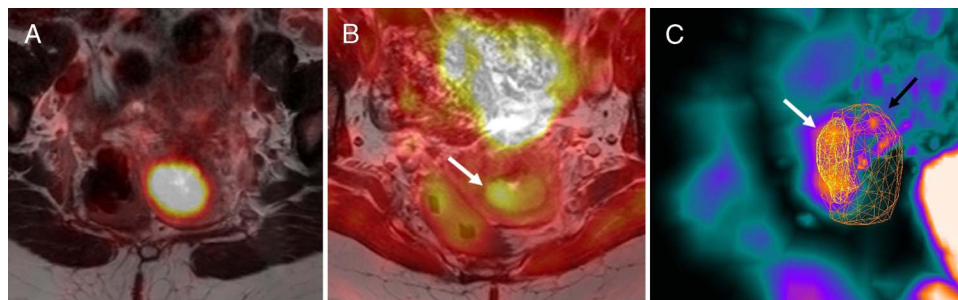
FIGURE 1. ^{18}F-EF5 and ^{18}F-FDG PET/MRI scans of patient 6. **A**, ^{18}F-FDG PET/MRI transaxial fused image shows the metabolically active cervical tumor. **B**, ^{18}F-EF5 PET/MRI (T2-weighted TSE) transaxial fused image (same level as in **A**) shows ^{18}F-EF5–avid area in the right side of the tumor (white arrow). **C**, In 3-dimensional ^{18}F-EF5 PET image, the solid yellow area (white arrow) represents the HS inside of ^{18}F-FDG positive tumor (black arrow).

TABLE 2. Localization of the Tumor Hypoxia in ^{18}F-EF5/FDG Imaging

Patient No.	Clinical FIGO Stage	No. Hypoxia Site	Anterior	Posterior	Middle	Superior	Inferior	Hypoxia in Periphery of FDG Tumor
1	1b1	1	−	−	−	+	−	+
2	1b2	2	+	+	−	−	+	+
3	1b2	1	+	−	−	+	+	+
4	2a1	>2	+	−	−	+	+	+
5	3a	>2	+	−	−	−	+	+
6	1b1	1	−	−	+	−	−	−
7	1b2	>2	+	+	+	−	+	+
8	2b	1	+	+	+	−	+	+
9	2a1	1	+	+	−	+	+	+
			Pos 7/9	Pos 4/9	Pos 3/9	Pos 4/9	Pos 7/9	Pos 8/9

1:8000), GLUT1 (GT12-A; Immune Diagnostics and Research, Hämeenlinna, Finland, 1:1000), and HIF1α (610959; BD Transduction Laboratories, Franklin Lakes, NJ, 1:100). The expression of the tissue sections was scored semiquantitatively using 5 to 10 visual fields with a 20× magnification microscope objective for plasma membrane expression (GLUT1 and CAIX) and for nuclear expression (HIF1α).

The percentage of positively stained tumor cells (0%–100%) was evaluated, and staining intensity was described as 1 = weak, 2 = moderate, or 3 = strong. Each tumor was scored (range = 0–300) by multiplying the average intensity value by the average percentage of positively stained cells. This IHC expression score was the numeric value for biological markers in comparison to other parameters and was reviewed previously.[10]

Statistical Analysis

Statistical analyses were performed using JMP Pro 14.1.0 for Windows version 10 (SAS Institute).

Descriptive statistics for the data are presented as mean ± standard deviation (SD).

The Pearson correlation among the PET imaging parameters, ICH hypoxia markers, and tumor size was examined. The 2-sample t test was used to correlate PET parameters with the tumor stage. Linear models for advanced tumor stage were also performed, adding tumor size to the model. Statistical significance was defined as P value <0.05 (2-tailed).

RESULTS

^{18}F-EF5/FDG Imaging and Location of Hypoxia

Nine primary cervical cancer patients were staged both clinically and according to diagnostic ^{18}F-FDG PET/MRI (Table 1). The ^{18}F-EF5 uptake was seen in all 9 tumors inside of the ^{18}F-FDG active area and in 2 widespread tumors even beyond with the highest HSV and PHA values (patients 4 and 8). The mean hypoxic area fraction in the ^{18}F-FDG active area was 28% ± 24%. Clinically, most stage I tumors confined to the uterus had a single hypoxic area. The distribution of hypoxia was heterogeneous with intratumor and intertumor variability. The location of hypoxia in all tumors was detected mainly in the periphery (8/9) and anterior-inferior parts (7/9) (Fig. 1). The location of the hypoxia and the results of different PET parameters such as MATV, HSV, PHA, and hypoxia markers are shown in Tables 2 and 3.

Tumor Hypoxia and Stage

The FIGO staging of carcinoma of the cervix uteri covers the assessment of tumor size and extension into the surrounding tissues, retroperitoneal lymph nodes, and adjacent/distant organs. In this study, HSV in ^{18}F-EF5 imaging correlated significantly with the maximum size of the tumor ($r = 0.72$, $P = 0.027$). In the advanced stage of cervical cancer with local and/or nodal disease in ^{18}F-FDG PET/MRI, the ^{18}F-EF5 max T/M ratio ($P = 0.036$) and HSV ($P = 0.040$) were significantly higher (mean max T/M ratio = 5.29 ± 0.94 g/mL, mean HSV = 8.33 ± 3.92 cm^3)

TABLE 3. PET Imaging Parameters and ICH Hypoxia Markers

| Patient No.	^{18}F-FDG PET/MRI		^{18}F-EF5 PET/MRI				Hypoxia Markers		
	SUV$_{max}$	Volume, MATV, cm^3	Max T/M, g/mL	Mean T/M, g/mL	Volume, HSV, cm^3	PHA %	HIF1α Score	CAIX Score	GLUT1 Score
1	3.1	1.1	2.4	2.5	0.2	17.6	NA	NA	NA
2	12.1	33.3	7.6	3.3	5.7	17.1	20	20	30
3	8.5	21.3	5.8	3.3	7.2	33.6	23	267	57
4	5.4	18.2	7.4	0.4	14.7	80.7	69	216	150
5	7.9	39.3	5.5	2.5	6.0	15.1	15	81	144
6	11.4	15.8	1.7	1.7	3.5	21.9	0	28	69
7	6.0	22.1	1.5	1.6	1.3	6.1	5	30	75
8	7.6	24.7	2.8	2.0	12.5	50.8	3	207	24
9	4.7	19.6	2.6	1.9	3.9	19.9	0	5	78
Mean ± SD	7.4 ± 3.0	21.7 ± 10.8	4.1 ± 2.4	2.1 ± 0.9	6.1 ± 4.8	28.3 ± 23.8	17 ± 23	107 ± 106	78 ± 47

NA, not available.
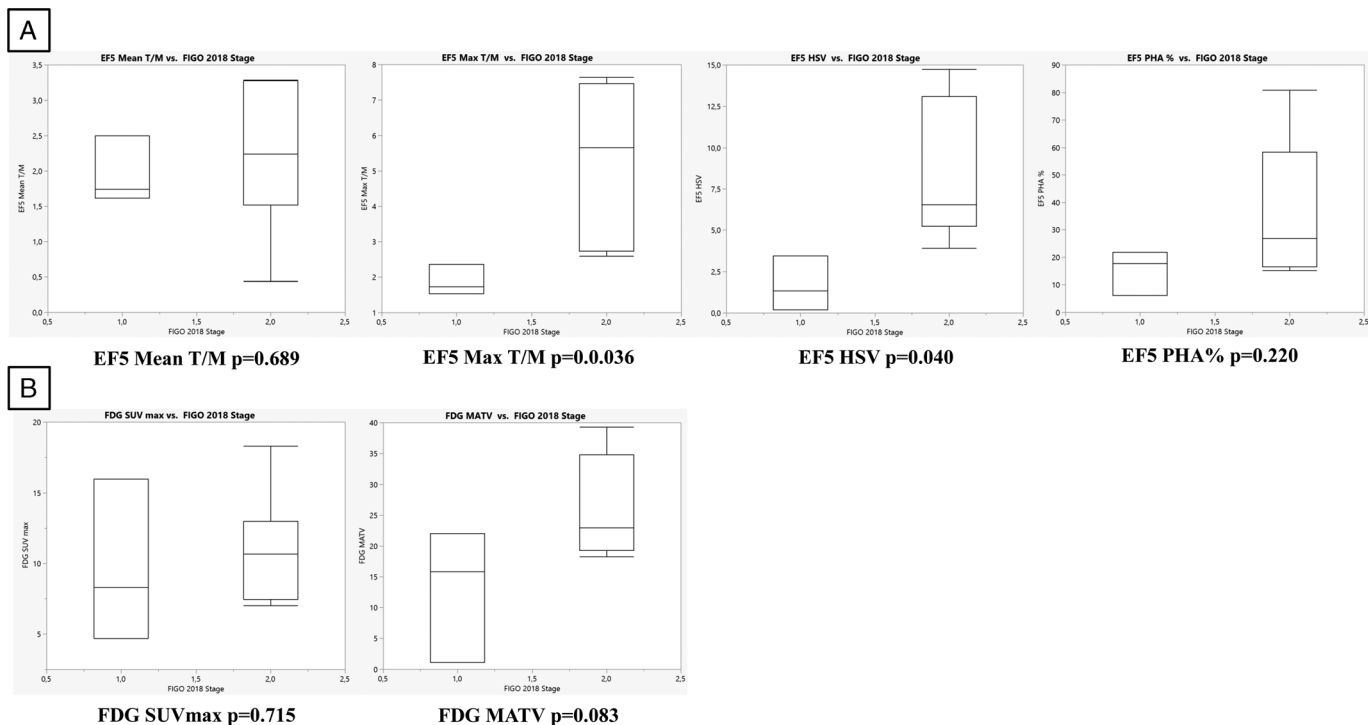
FIGURE 2. Correlation between ^{18}F-EF5 and ^{18}F-FDG values and stage. **A**, Correlations between ^{18}F-EF5 values and FIGO 2018 stage I versus stage II to IV cervical cancer. **B**, Correlations between ^{18}F-FDG values and FIGO 2018 stage I versus stage II to IV cervical cancer.
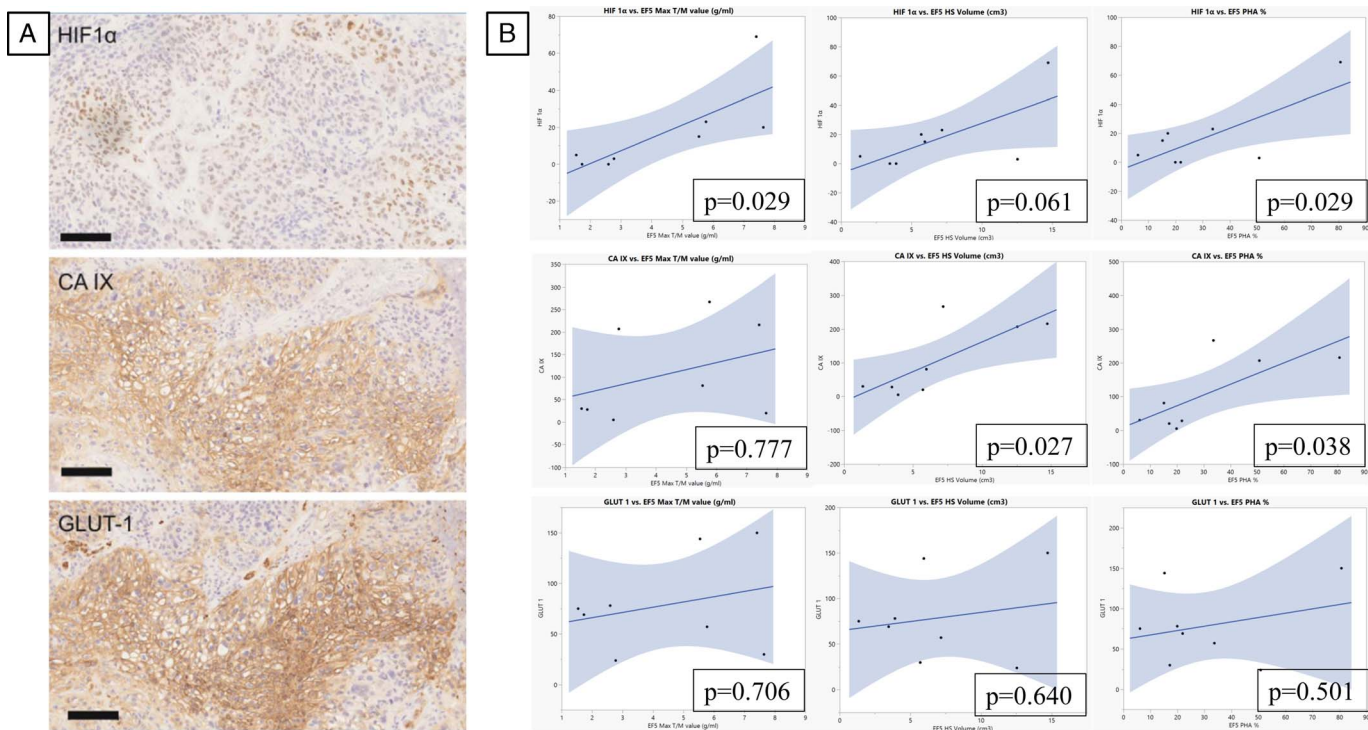

FIGURE 3. Hypoxia immunohistochemistry markers and ^{18}F-EF5 values. **A**, Immunohistochemistry expression for HIF1α, CAIX, and GLUT1 in fresh biopsies of SCC cervix, patient 6. Nuclear expression of HIF1α was weak, and plasma membrane expression GLUT1 and CAIX was moderate (20× magnification, scale bar 100 μm). **B**, Correlations between ^{18}F-EF5 values and immunohistochemistry markers.

than in stage I disease (mean max T/M ratio = 1.87 ± 0.35 g/mL, mean HSV = 1.66 ± 1.35 cm^3), and this finding was independent from tumor size in linear modeling (data not shown). The same trend was found with locally advanced tumors and high HSV (P = 0.073). Instead, ^{18}F-FDG values did not correlate with these stages of cervical cancer (Fig. 2).

^{18}F-FDG PET/MRI detected lymph node metastases (LNMs) in the pelvic area in 3 patients and in the para-aortic area outside the ^{18}F-EF5 imaging field in 1 patient. Only one large peritumoral LNM was also ^{18}F-EF5 avid with PHA 6.3% (patient 5). The MATV of this LNM was high (13.1 cm^3) compared with the other LNM, in which MATV ranged between 1.0 and 3.4 cm^3. In all patients, the primary tumor MATV value (P = 0.036) and the ^{18}F-EF5 mean T/M ratio (P = 0.047) correlated significantly with the presence of LNM.

Tumor Hypoxia and Immunohistochemistry

The immunostaining in the tumor fresh biopsies displayed a heterogeneous expression pattern, with the lowest values in HIF1α. ^{18}F-EF5 max T/M ratio correlated statistically significantly with HIF1α and HSV with CAIX. PHA was correlated with both HIF1α and CAIX. The correlation of GLUT1 expression with ^{18}F-EF5 values did not reach statistical significance in this small cohort (Fig. 3). ^{18}F-FDG PET/MRI displayed visible radiotracer uptake in all patients. The ^{18}F-FDG values did not correlate with the ^{18}F-EF5 values or the ICH hypoxia markers.

DISCUSSION

In this prospective pilot study, we investigated the potential of ^{18}F-EF5 PET/MRI to detect tumor hypoxia in patients with primary SCC of the cervix uteri. In locally advanced cancer, multiple ^{18}F-EF5– avid areas were visible, whereas clinical stage I tumors presented mostly in one homogenous region. We observed that tumor hypoxia is typically localized in the periphery of the tumor, reflecting the common clinical presentation of cervical SCC as exophytic local tumor extension and weaker vasculature in tumor edges. These findings are in line with earlier studies of in situ EF5 binding in SCC tumors, where intratumoral heterogeneity was largest in tumors with high EF5 binding regions, and blood vessels were at a distance from those regions.[11]

The presence of hypoxia in tumors has been associated with chemotherapy and radiotherapy resistance, possibly due to reduced drug penetration. Up to 50% to 60% of locally advanced solid tumors may present hypoxic areas that are heterogeneously distributed.[8] This was also seen in our material, especially in locally advanced tumors with high HSV and PHA. In 2 of 9 patients with these highest values, the hypoxic regions localized even outside the ^{18}F-FGD active area. Zegers et al[12] reported an average 24% of the total hypoxic volume located outside the ^{18}F-FDG high volume in non–small cell lung cancer primary tumors using ^{18}F-flortanidazole (HX4) and ^{18}F-FDG imaging. The heterogeneity of hypoxia areas on a tumor-to-tumor basis emphasizes the need to optimize tumor imaging to personalize the therapy. In our study, there was a lack of correlations between ^{18}F-EF5 and ^{18}F-FDG uptake, which was expected from previous studies of cervical cancer and other tumors with different hypoxia PET tracers and confirms the unique information achievable from PET hypoxia imaging.[1,13,14]

Our study indicates that ^{18}F-EF5 PET/MRI may offer new diagnostic value for detecting local and nodal tumor spread in patients with primary cervical cancer. We found that exogenous hypoxia parameters ^{18}F-EF5 max T/M ratio and HSV correlated with tumor staging, lending support to advanced cancers being more hypoxic than stage I tumors. To date, only a few studies have investigated clinical PET imaging of tumor hypoxia in primary cervical cancer,[15] and many of them have reported an association with poor outcome.[13,14,16] In our data, the hypoxic volume in ^{18}F-EF5 imaging correlated with tumor size, which is in line with the study by Han et al.[17] They studied 27 cervical cancer patients with ^{18}F-fluoroazomycin arabinoside (ZAZA)

PET imaging and found, in agreement with the present study, that tumor volume correlated with HSV but not with PHA.

The correlation between metastatic regional lymph nodes and hypoxia is controversial. In cervical cancer, [60]Cu-ATSM uptake in the primary tumor correlated with LNM, whereas in head and neck cancer primary tumor, ^{18}F-EF5 uptake lacked correlation.[6,14] We found that ^{18}F-EF5 mean T/M ratio and MATV in the cervix tumor correlated with the presence of LNM, and the anatomically largest LNM was particularly hypoxic with ^{18}F-EF5 uptake. Thus, the volume of metabolically active cancers seems to indicate an increased potential to metastasize.

We validated the presence of PET-derived tumor hypoxia with IHC hypoxia markers in fresh tumor biopsies taken from the edges of cervical cancer. There was a significant correlation between the endogenous hypoxia markers HIF1α and CAIX and exogenous ^{18}F-EF5 PET imaging parameters. To our knowledge, this evaluation of clinical cervical cancer patients has not been reported before, but a similar correlation between these hypoxia markers and high ^{18}F-EF5 uptake was seen in head and neck squamous cell carcinoma xenografts.[10] Also, association between overexpression of CAIX and hypoxic cervical cancer tumors in [60]Cu-ATSM PET imaging has been documented.[16] The main challenge with tumor biopsies, however, is that they represent only tiny biopsied areas, not the whole tumor, which impedes the use of tumor biopsies in detecting heterogeneous tumor hypoxia. Also, IHC detection of HIF1α can be difficult due to the short half-life and may partly explain the low levels of expression scores in our data.

The strength of this prospective pilot study is the use of PET/ MRI with ^{18}F-EF5 tracer to investigate hypoxia noninvasively together with the endogenous hypoxia markers in cervical cancer. The small sample size can be considered a limitation of our pilot study. Further, the labeling chemistry of EF5 is complex and may restrict the broader use of this tracer.

In conclusion, we demonstrated that ^{18}F-EF5 PET/MRI can detect hypoxia in primary cervical SCC with multiple EF5-avid areas in more advanced cancers. The intensity and size of hypoxia correlated with tumor stage. This method could be useful in developing hypoxia-targeted therapies, such as optimizing chemoradiation and finding the most aggressive tumors with hypoxia.

REFERENCES

1. Challapalli A, Carroll L, Aboagye EO. Molecular mechanisms of hypoxia in cancer. *Clin Transl Imaging.* 2017;5:225–253.

2. Wouters BG, Weppler SA, Koritzinsky M, et al. Hypoxia as a target for combined modality treatments. *Eur J Cancer.* 2002;38:240–257.

3. Nguyen NC, Beriwal S, Moon CH, et al. Diagnostic value of FDG PET/MRI in females with pelvic malignancy—a systematic review of the literature. *Front Oncol.* 2020;10:519440.

4. Koch CJ, Scheuermann JS, Divgi C, et al. Biodistribution and dosimetry of ^{18}F-EF5 in cancer patients with preliminary comparison of ^{18}F-EF5 uptake versus EF5 binding in human glioblastoma. *Eur J Nucl Med Mol Imaging.* 2010;37:2048–2059.

5. Dolbier WR, Li AR, Koch CJ, et al. ^{18}F-EF5, a marker for PET detection of hypoxia: synthesis of precursor and a new fluorination procedure. *Appl Radiat Isot.* 2001;54:73–80.

6. Komar G, Seppänen M, Eskola O, et al. ^{18}F-EF5: a new PET tracer for imaging hypoxia in head and neck cancer. *J Nucl Med.* 2008;49:1944–1951.

7. Komar G, Lehtiö K, Seppänen M, et al. Prognostic value of tumour blood flow, ^{18}F-EF5 and ^{18}F-FDG PET/CT imaging in patients with head and neck cancer treated with radiochemotherapy. *Eur J Nucl Med Mol Imaging.* 2014; 41:2042–2050.

8. Vaupel P, Mayer A. Hypoxia in cancer: significance and impact on clinical outcome. *Cancer Metastasis Rev.* 2007;26:225–239.

9. Eskola O, Grönroos TJ, Forsback S, et al. Tracer level electrophilic synthesis and pharmacokinetics of the hypoxia tracer ^{18}F-EF5. *Mol Imaging Biol.* 2012;14:205–212.

10. Silén J, Högel H, Kivinen K, et al. Uptake of ^{18}F-EF5 as a tracer for hypoxic and aggressive phenotype in experimental head and neck squamous cell carcinoma. *Transl Oncol.* 2014;7:323–330.

11. Evans SM, Hahn S, Pook DR, et al. Detection of hypoxia in human squamous cell carcinoma by EF5 binding. *Cancer Res.* 2000;60:2018–2024.

12. Zegers CML, van Elmpt W, Reymen B, et al. In vivo quantification of hypoxic and metabolic status of NSCLC tumors using ^{18}F-HX4 and ^{18}F-FDG PET/CT imaging. *Clin Cancer Res.* 2014;20:6389–6397.

13. Dehdashti F, Grigsby PW, Lewis JS, et al. Assessing tumor hypoxia in cervical cancer by PET with ^{60}Cu-labeled diacetyl-bis(N4-methylthiosemicarbazone). *J Nucl Med.* 2008;49:201–205.

14. Vercellino L, Groheux D, Thoury A, et al. Hypoxia imaging of uterine cervix carcinoma with ^{18}F-FETNIM PET/CT. *Clin Nucl Med.* 2012;37:1065–1068.

15. Lyng H, Malinen E. Hypoxia in cervical cancer: from biology to imaging. *Clin Transl Imaging.* 2017;5:373–388.

16. Grigsby PW, Malyapa RS, Higashikubo R, et al. Comparison of molecular markers of hypoxia and imaging with ^{60}Cu-ATSM in cancer of the uterine cervix. *Mol Imaging Biol.* 2007;9:278–283.

17. Han K, Shek T, Vines D, et al. Measurement of tumor hypoxia in patients with locally advanced cervical cancer using positron emission tomography with ^{18}F-Fluoroazomyin arabinoside. *Int J Radiat Oncol Biol Phys.* 2018;102:1202–1209.